ADVANCED MATERIALS INTERFACES
www.advmatinterfaces.de

A Simple and Robust Method to Prepare Polyelectrolyte Brushes on Polymer Surfaces

Maiko Schulze, Seyma Adigüzel, Philip Nickl, Ann-Cathrin Schmitt, Jens Dernedde, Matthias Ballauff, and Rainer Haag**

A simple and robust method is presented to immobilize a heparin-analog polyelectrolyte on inert hydrophobic surfaces. It is demonstrated that an amphiphilic block copolymer consisting of linear polyglycerol sulfate (lPGS) and a benzophenone modified anchor block can be bound to polystyrene surfaces in a facile dip-coating procedure. The chaotropic salt guanidinium chloride is used to overcome the aggregation of the polymer as well as the repulsion between highly hydrated sulfate groups and the polystyrene surface. Irradiation with UV light tethers the polymer chains covalently to the surface. The resulting coating exhibits an aggregate morphology that resembles the aggregation behavior in solution, with a coating thickness of 8 nm. The behavior of the surfaces is dominated by the polyelectrolyte brush coating. They swell and collapse in response to different ionic strengths of the surrounding medium, and bind proteins via electrostatic interactions. The coating is stable toward physiological conditions over the course of several weeks. Coated surfaces bind to proteins of the complement cascade when in contact with dilute blood serum, which results in a decrease of complement activity to 78 ± 4%. The coating procedure can also be applied to other non-activated polymer surfaces, as demonstrated on a polypropylene fleece.

1. Introduction

When biomaterials or medical devices get in contact with tissue or blood, proteins will adsorb to their surface within seconds.[1,2] Highly mobile proteins adsorb immediately, followed by a series of rearrangements and displacements by proteins with higher binding affinity.[3] This rapid process initiates several biological reactions, including activation of the coagulation cascade and the complement system, which will lead to blood clotting and inflammatory responses.[4–6] However, the material of medical devices is usually chosen for their bulk properties, e.g., a desired combination of flexibility and strength, rather than their surface properties.[4,5] Hence, many blood-contacting devices like vascular grafts are made of polymeric materials, e.g., silicones or polyurethanes and the hydrophobicity of such materials is the main driving factor for high protein adsorption.[6,7]

A vast amount of research has been focused on reducing protein adsorption by making the surface of such materials more hydrophilic. An important approach is a functionalization with hydrophilic polymers like polyethylene glycol (PEG), which repels proteins due to its strongly bound hydration shell and steric repulsion effects.[8–10] PEG has found widespread uses already, in medical fields as well as the cosmetics and food industry. The vast range of applications has led to a rising number of individuals who developed antibodies against PEG, lowering the efficacy of PEG in medical applications, or even causing adverse effects like hypersensitivity reactions.[11–14]

Mimicking the biological function of the endothelium by immobilizing heparin on the surface is another approach to increase blood compatibility.[15] The carbohydrate heparin is structurally closely related to heparan sulfate, a major constituent of the vascular endothelium and the extracellular matrix that plays a role in binding and storage of clotting factors as well as components of the immune system.[16] As biological molecules, these linear polyelectrolytes need to be extracted from animal tissue and therefore carry the intrinsic problem of possible contaminations with infectious materials. The primary source for heparin in the USA has been tissue from cattle, until these products had to be replaced in the 1990s due to the possibility of prion contamination from cattle infected with bovine spongiform encephalopathy (BSE).[17] Porcine intestines have been a reliable source for heparin since then, but other diseases like African swine fever remain a threat to the global heparin production.[18] Furthermore, heparin and heparan sulfate are

M. Schulze, S. Adigüzel, P. Nickl, A.-C. Schmitt, M. Ballauff, R. Haag
Institute of Chemistry and Biochemistry
Freie Universität Berlin
Takustr. 3, 14195 Berlin, Germany
E-mail: mballauff@zedat.fu-berlin.de; haag@chemie.fu-berlin.de
J. Dernedde
Institute of Laboratory Medicine
Clinical Chemistry and Pathobiochemistry
Charité – Universitätsmedizin Berlin
CVK
Augustenburger Platz 1, 13353 Berlin, Germany
The ORCID identification number(s) for the author(s) of this article can be found under https://doi.org/10.1002/admi.202102005.

DOI: 10.1002/admi.202102005

generally a diverse mixture of similar compounds and need to undergo extensive purification steps in order to achieve a uniform sample.[19]

Synthetic polyelectrolytes that mimic the biological function of heparin and heparan sulfate can be a useful tool to avoid the intrinsic risks of heparin.[7,20,21] Polyglycerol sulfate may be a suitable candidate for that purpose, since it has been introduced as a replacement for heparin.[22] In the last decade, this polymer class has been investigated extensively in solution, demonstrating that it can reduce inflammation in vitro and in vivo.[23–25] However, surfaces coated with polyglycerol sulfate have scarcely been reported so far. Stöbener et al. immobilized a thioctic acid-functionalized form of hyperbranched polyglycerol sulfate (hPGS) on gold substrates and investigated the adsorption of the proteins albumin and fibrinogen. They applied the quartz crystal microbalance with dissipation (QCM-D) and found that electrostatic interactions between positively charged patches and domains on the proteins and the negatively charged sulfate groups on the polymer lead to binding of both proteins.[26] The electrostatic nature of protein adsorption to polyelectrolyte-coated surfaces and their dependence on the ionic strength of the surrounding medium has been confirmed by Walkowiak et al. in another QCM-D based study, utilizing polyacrylic acid brushes and albumin.[27] Both studies demonstrate the activity of the respective polyelectrolytes on a surface. However, there is still a gap between such model studies on gold surfaces and possible applications on biomedical devices.

A special challenge that needs to be faced when coating polymeric material surfaces is their sensitivity toward organic solvents. Grafting polyelectrolytes by surface-initiated polymerization usually leads to a high coating density and controllable layer thickness, but is often performed in organic solvents, with only a few examples working under aqueous conditions.[27–31] Grafting-to approaches can be applied in water for amphiphilic polymers, but due to steric and electrostatic repulsion of the charged polymers, it is difficult to achieve a grafting density high enough to show sufficient activity for the respective application.[32]

In this study, we aim to develop a simple and robust method to produce polyelectrolyte brush coatings with polyglycerol sulfate that can be applied to nonactivated polymer material surfaces via a dip-coating method. The resulting coating should exhibit characteristic properties of a polyelectrolyte brush coating, including binding proteins via electrostatic interactions, and it should demonstrate an increased hemocompatibility by reducing the complement activity of contacting blood serum.

2. Results and Discussion

2.1. Synthesis

The design of the polymer used in this study is related to the coating method by Yu et al.[33] It consists of a functional linear block of polyglycerol sulfate (lPGS) and a short anchor block, also based on linear polyglycerol, but functionalized with benzophenone (BPh) groups, which can bind reversibly to hydrophobic surfaces and can be crosslinked with the surface via UV light irradiation. The synthesis of the block copolymer lPGS-b-BPh consists of two synthetic steps, starting from the polymer lPG-b-NH_2 (**Scheme 1**).[34] Functionalization of the amine block by amide coupling with a carboxylic acid derivative of benzophenone with 1-ethyl-3-carbodiimide hydrochloride (EDC) and *N*-hydroxysuccinimide (NHS) in *N,N*-dimethylformamide (DMF) resulted in 4% benzophenone content. The sulfation was carried out according to a modified standard protocol, utilizing a sulfur trioxide pyridine complex in DMF under dry conditions, yielding a degree of sulfation of over 90%.[22] Pyridinium ions were removed from the polymer by dialysis against concentrated aqueous NaCl solution at pH = 8.

The reaction sequence made sure that the remaining free amino groups will be sulfated as well. This allowed to avoid positively charged groups in the polymer that would potentially form ionic pairs with the sulfate groups and affect the conformation or aggregation behavior in an aqueous solution.

2.2. Behavior in Aqueous Solution

Considering the amphiphilic character of the polymer lPGS-b-BPh, we assumed that it would bind via hydrophobic interactions to surfaces like polystyrene. However, no significant interactions could be observed in QCM-D online coating experiments (see Figure S3, Supporting Information) and no coating was found when performing offline coating experiments on polystyrene surfaces. Dynamic light scattering measurements (DLS) revealed that the polymer forms stable aggregates in aqueous solution, even at the lowest concentration that could be measured reliably by the DLS instrument (**Figure 1**A). It seems likely that the aggregation influences the adsorption process since the BPh moieties are hidden inside the aggregates. Additionally, sulfate groups form a strong hydration shell and avoid interactions with hydrophobic surfaces. In Yu's study, the nonsulfated analog of lPGS-b-BPh did not aggregate under similar conditions and adsorbed efficiently to polystyrene.[33]

We found that the aggregation of lPGS-b-BPh, made visible in cryo-transmission electron microscopy (CryoTEM, see Figure 1B and Figure S4, Supporting Information) by replacing the Na^+ ions within the polymer by Cs^+ ions for better contrast, could not be circumvented by applying heat, ultrasonication, or by adding organic solvents like ethanol, dimethyl sulfoxide or DMF. Evidently, the aggregation behavior was strong enough to withstand common factors relevant for hydrophobic interactions. Further experiments demonstrated that the addition of different salts has a significant impact on the observed particle size in DLS (Figure 1C,F). Every tested salt reduced the observed hydrodynamic diameter, in accordance with a collapse of the polyelectrolyte chains as response to the increased ionic strength.[35] However, the extent of this effect varies between the salts. A systematic comparison of different cations and different anions showed that the extent of their effect can be roughly related to the Hofmeister series.[36] The Hofmeister series, originally reported by Franz Hofmeister in 1888, describes how different ions influence the stability and solubility of amphiphilic molecules in aqueous solution.[37] Chaotropic salts can increase the solubility of hydrophobic domains and thereby increase

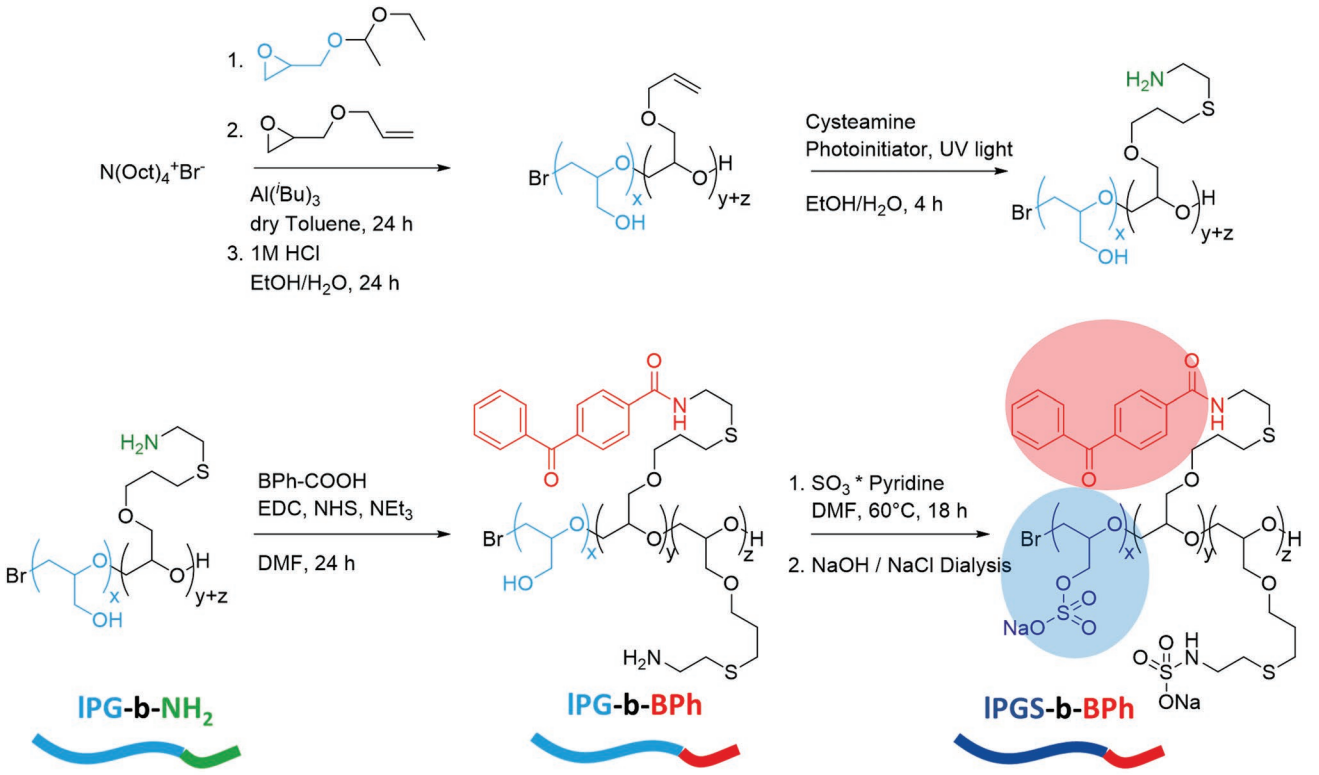

Scheme 1. The starting polymer lPG-b-NH_2 was synthesized according to a previously published method.[33] In brief, one acetal protected and one allyl functionalized glycidyl ether were copolymerized successively ($x = 110$, $y + z = 10$). Next, the acetals were hydrolyzed under acidic conditions and the allyl groups were postmodified with cysteamine in a thiol–ene-click reaction. Benzophenone moieties are then coupled to the amino groups by an amide coupling procedure in DMF using EDC and NHS as coupling reagents. The reaction reliably yielded about 4% benzophenone content in the final polymer. Subsequently, treatment with a sulfur trioxide–pyridine complex under dry conditions in DMF converts the free alcohol groups into sulfates as well as the remaining amino groups into amidosulfones. Pyridine was removed by dialysis in concentrated NaCl solution under slightly basic conditions to yield the final polymer lPGS-b-BPh with a degree of sulfation of >90%.

the overall solubility of the compound, while decreasing the conformational stability. Kosmotropic salts decrease the solubility of hydrophobic domains and of the compounds' overall solubility but increase the conformational stability.

The salt species tested in this experiment are in the order of kosmotropic (on the left) to chaotropic (on the right). A general trend towards lower hydrodynamic diameters was observed for chaotropic salts, indicating that the chaotropic character destabilizes the aggregates and thereby reduces their size. A chaotropic salt will therefore be added to the polymer solution during the coating procedure.

2.3. A Chaotropic Salt Enables Successful Coating on PS

The addition of chaotropic salts to an aqueous solution of lPGS-b-BPh changes the aggregate size. This effect will now be used for a successful coating on surfaces of PS (**Figure 2**). Since guanidinium chloride (GHCl) showed the lowest observed hydrodynamic diameter in DLS experiments (see Figure 1), it was employed for the following coating experiments as shown in Figure 2.

In a QCM-D experiment, a good adsorption of the polymer to the PS surface was observed. This was deduced from the negative frequency shift, representing a mass increase on the sensor surface. The dissipation shift increases slightly in that process, showing that the adsorbed layer of lPGS-b-BPh adds only little to the viscoelasticity of the surface. Washing with the salt solution demonstrated that most of the polymer was tightly adsorbed to the surface. The process of UV crosslinking by irradiation at 366 nm for 10 min and subsequent further washing had no significant impact on the adsorbed mass. In the last step, salt-free water was applied to the coated surface, leading to a drastic negative frequency shift and positive dissipation shift. This observation corresponds to the reorientation of the polyelectrolyte from the salted brush to the osmotic brush regime, as will be discussed in greater detail in Section 2.4. Hence, this coating experiment proves that the polymer can be adsorbed and covalently attached to the PS surface in a simple procedure.

The necessity of benzophenone moieties for a good adsorption was demonstrated in a control experiment employing a block-copolymer that does not contain benzophenone (lPGS-b-NH_2). The QCM-D experiment was performed under analogous conditions, including addition of GHCl (Figure S5, Supporting Information). The binding of lPGS-b-NH_2 to PS is reduced about 80% as compared to lPGS-b-BPh and is likely a result of pure electrostatic interactions between guanidinium ions adsorbed to PS and sulfate groups on the polymer. Furthermore, the UV crosslinking step is crucial for the stability of the coating. When this step is left out in the coating procedure,

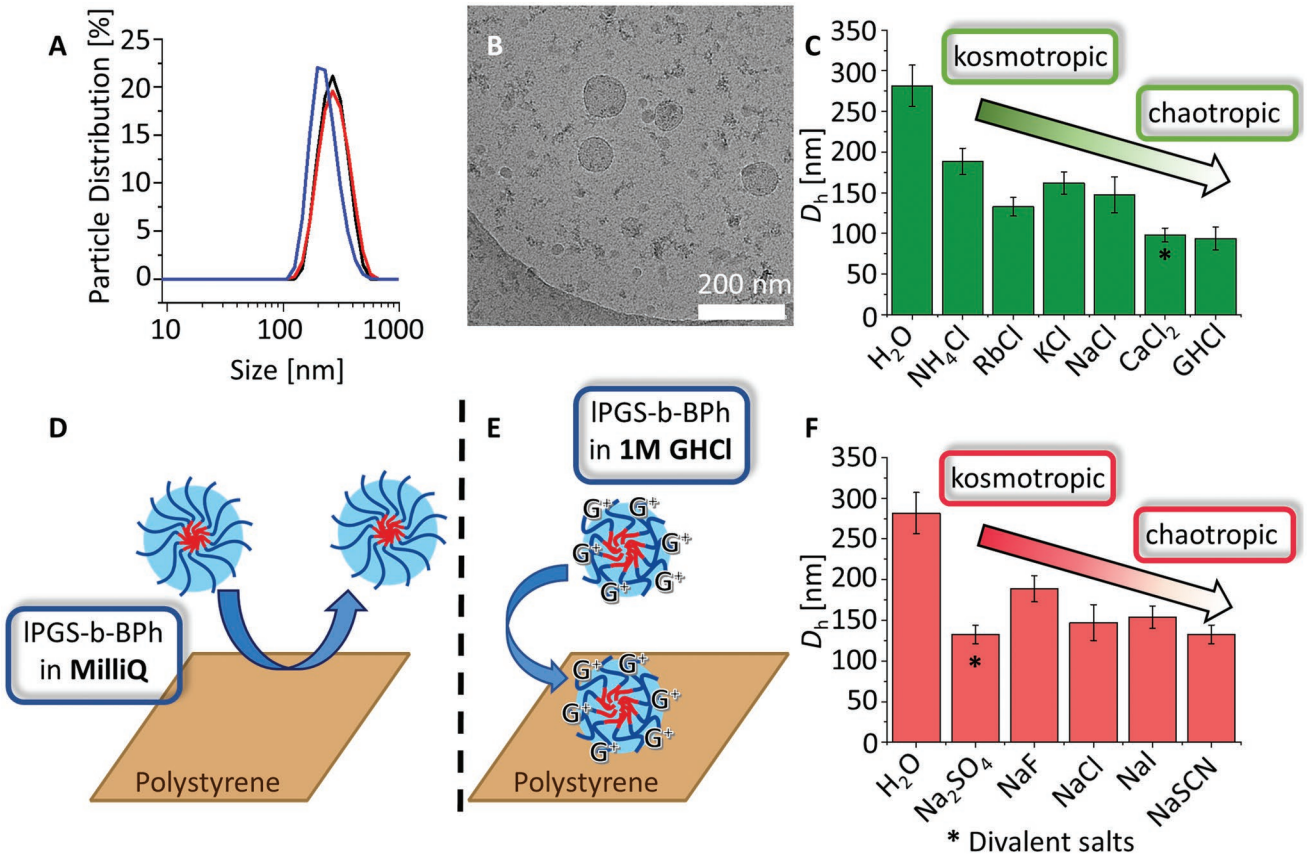

Figure 1. Behavior of lPGS-b-BPh in aqueous solution. A) lPGS-b-BPh shows aggregates with a hydrodynamic diameter of about 200 nm in water in DLS measurements (c = 0.1 mg mL^{-1}, T = 20 °C, red: intensity distribution, black: volume distribution, blue: number distribution). B) In Cryo-TEM, aggregates of different sizes and shapes are observed (c = 1 mg mL^{-1}, the Na^+ counterions of lPGS-b-BPh have been replaced by Cs^+ for better contrast). C,F) The hydrodynamic diameter of the polymer aggregates is reduced by adding salts ($c_{Polymer}$ = 0.1 mg mL^{-1}, c_{Salt} = 0.1 mol L^{-1}, T = 20 °C). The salt species are in order of the Hofmeister series, from kosmotropic on the left to chaotropic on the right. Chaotropic salts show a stronger size reduction of the aggregates than kosmotropic salts. A systematic comparison of different cations is depicted in C, of different anions in F. * Divalent salt species show increased size reduction due to their higher ionic strength at equal salt concentration. D,E) Schematic representation of how chaotropic ions may change the adsorption behavior to hydrophobic surfaces (G^+ represents guanidinium ions). The increased ionic strength leads to the collapse of the polyelectrolyte chains. The chaotropic character may destabilize the aggregate and allow hydrophobic interactions with the surface.

most of the polymer will quickly be detached from the PS surface during washing with MilliQ water (Figure S5, Supporting Information).

Next, the coating procedure was transferred onto silicon wafers coated with polystyrene. The wafers were coated by incubating them with 1 M GHCl solution, followed by the polymer solution, thorough washing with salt solution, and then crosslinking under UV light. The coating success was characterized by means of atomic force microscopy (AFM), ellipsometry, and contact angle measurements after further washing with buffer and MilliQ water. Organic solvents were tested in the coating procedure as well, but had no significant effect on the outcome of the coating experiments (Table S1, Supporting Information).

Atomic force microscopy images on dried surfaces revealed that the coated surfaces show an aggregate morphology, which resembles the aggregation behavior in solution (Figure 2B, additional images in Figures S6 and S8, Supporting Information). The PS surface was covered in patches of polymer with an average diameter of 80 nm, the average height of 8 nm, and overall coverage of about 50%. The coating thickness determined by ellipsometry was (1.7 ± 0.3) nm, averaging overcoated as well as empty areas. The static water contact angle was (75 ± 3)° (Figure S6, Supporting Information) and the captive bubble contact angle was (72 ± 2)° (Figure S7, Supporting Information). Since the polyelectrolyte chains are expected to swell significantly in the presence of water, additional AFM measurements have been performed to compare a surface in dried and in wet state. Upon applying water, a smooth and flat surface was observed (Figure S9, Supporting Information). This observation shows that the polyelectrolyte chains stretch out and fully cover the underlying PS surface in wet state.

Overall, it could be demonstrated that adding a chaotropic salt can change the behavior of lPGS-b-BPh in aqueous solution to such an extent that it can adsorb to a PS surface. On the surface, the benzophenone groups in the anchor block can be activated by UV irradiation and crosslink with the surface. The presented procedure allows the production of polyelectrolyte layers on PS in a facile and robust way.

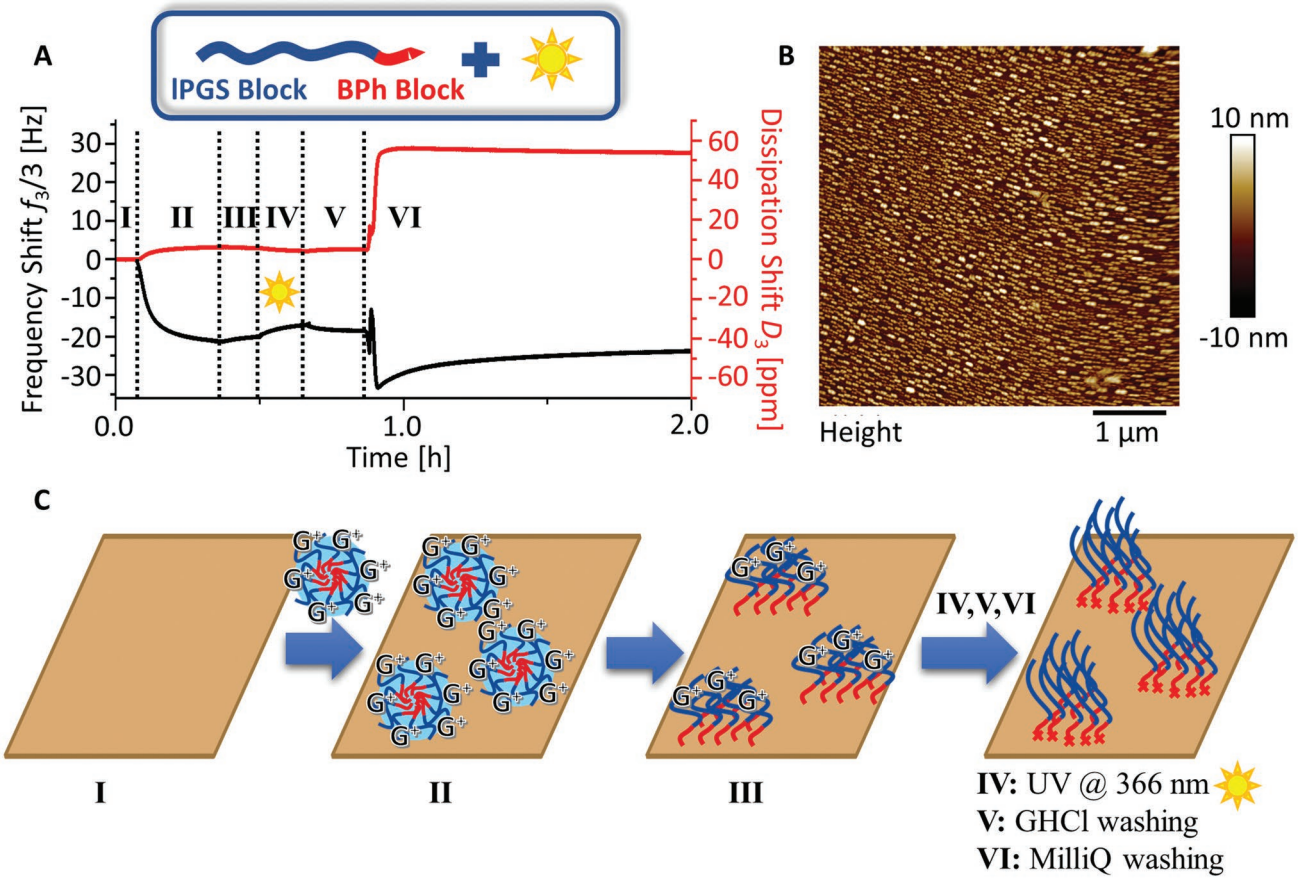

Figure 2. Coating behavior of lPGS-b-BPh in presence of the chaotropic salt guanidinium chloride (GHCl). A) QCM-D measurement of the coating process. A polystyrene coated sensor surface is equilibrated in 1 M GHCl solution (I), then lPGS-b-BPh is added (II, 0.1 mg mL^{-1} in 1 M GHCl solution), followed by washing with the salt solution (III), irradiation with UV light (IV, 10 min at 366 nm), further washing (V), and subsequently washing with MilliQ water (VI). The adsorption of the polymer to the surface is clearly visible in step II, as indicated by the negative frequency shift. Washing with water in step VI leads to a conversion from the salted brush regime to osmotic brush regime. In that process, the mass of the layer is increased due to water uptake, which leads to a negative frequency shift. Furthermore, the stretching of the brushes increases the viscoelasticity of the surface drastically, leading to a strong positive dissipation shift. B) The coated surface shows an aggregate morphology in AFM measurements, resembling the aggregation behavior in solution. C) Proposed coating mechanism. In presence of guanidinium ions, lPGS-b-BPh aggregates can adsorb to polystyrene and form a brush-like coating after reorganization and UV crosslinking. Roman numerals refer to the respective step in A.

2.4. Characterization of Coated Surfaces

Next, the response of the coated surface to different ionic strengths is investigated. As highly charged molecules, the conformation of a strong polyelectrolyte like lPGS is dependent on the ionic strength of the surrounding medium. In a QCM-D experiment, a precoated sensor surface was repeatedly exposed to buffer solutions of different ionic strengths (**Figure 3**).

Starting at $I_{(I)} = 50 \times 10^{-3}$ M, the ionic strength was increased in steps of 25×10^{-3} M up to $I_{(V)} = 150 \times 10^{-3}$ M. For each step it could be observed that the frequency shift was increased, indicating a water loss in the polymer layer. Simultaneously, the dissipation exhibited a negative shift, indicating a loss of viscoelasticity of the layer, which is caused by a partial collapse of the lPGS chains. The following stepwise decrease of ionic strength back to $I_{(I)} = 50 \times 10^{-3}$ M led to the opposite behavior, i.e., water uptake and polymer stretching. This procedure was repeated twice to demonstrate the reversibility of the system. Furthermore, the state of the system at different ionic strength was independent of going through the intermediate stages, as demonstrated by switching between $I_{(I)}$ to $I_{(V)}$ directly.

Evidently, the coating must be stable under physiological conditions (usually salt concentrations of about 150×10^{-3} M) for days, or up to several weeks. The stability of lPGS-b-BPh on PS surfaces was tested by applying different media that exert even higher stress than physiological salt concentrations. The surfaces were immersed for 4 weeks in either phosphate buffer (PB) with an ionic strength of $I = 50 \times 10^{-3}$ M, or MilliQ water, or a 2% detergent solution (sodium dodecylsulfate, SDS). After the incubation, X-ray photoelectron spectroscopy (XPS) analysis and atomic force microscopy (AFM) were performed (**Figure 4**).

Sulfur and nitrogen contents in the spectra indicate the presence of lPGS-b-BPh, as can be seen in the control measurement. Nitrogen results from the amidosulfone and amide groups in the polymer, while sulfur is present within the sulfate groups and, to a smaller extent, in the thioethers of the benzophenone block. The presence of lPGS-b-BPh on the surface was still confirmed after incubation for up to 4 weeks with PB

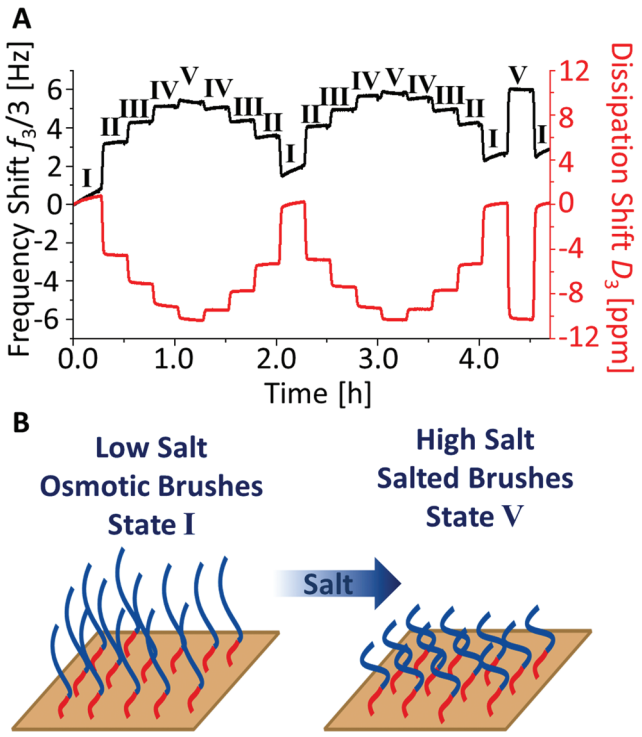

Figure 3. QCM-D experiment showing the response of a coated surface to different salt concentrations. A) Frequency and dissipation shift of a coated sensor in the presence of buffer solutions with different ionic strength. The ionic strength was increased stepwise via steps of 25×10^{-3} M from step I (50×10^{-3} M) to step V (150×10^{-3} M) and back two times. At low ionic strength, the brushes are in the extended osmotic regime. At high ionic strength, water is released and the brushes are in the collapsed salted regime. B) Schematic depiction of the osmotic brush and salted brush state of the lPGS coating at low ionic strength and high ionic strength, respectively.

or water. However, the sample incubated with 2% SDS solution did not show any remaining nitrogen content, indicating that the polymer has been removed from the surface. Sulfur atoms were still detectable but may also originate from SDS molecules adsorbed on the PS surface.

AFM measurements further supported these observations (Figure 4B,C). In phase images, it is clearly visible that the PB and MilliQ incubated surfaces still contained polymer coating, although the morphology had been changed due to the exposure to high osmotic pressure. The SDS incubated sample was distinct from the lPGS-b-BPh coated control, and rather resembled the uncoated PS surface (Figure S10, Supporting Information). It seems reasonable that the surface coating did not withstand the harsh conditions in this case, considering that the high osmotic pressure will lead to a strong stretching of the brushes. Here, the extended polymer chains will also pull on the polystyrene chains that they have been tethered to. The loosened PS chains could then be detached from the surface by interactions with SDS.

Based on the stability experiments, it seems reasonable to assume that regular physiological conditions, i.e., an ionic strength of about 150×10^{-3} M, would not affect the coating significantly. Even the high osmotic pressure in the osmotic regime obtained by washing the surface with MilliQ water did not remove the polymer from the surface. Only the addition of a strong detergent led to the removal of the lPGS-b-BPh layer, likely by detaching the polymer including the underlying polystyrene chains.

2.5. Protein Binding to Coated Surfaces Is Charge and Salt Dependent

The interactions of lPGS-b-BPh coated surfaces with two different proteins were investigated by QCM-D measurements. Sensor crystals with a PS surface have been precoated with lPGS-b-BPh in an offline coating procedure. They were then exposed to either human serum albumin (HSA) or lysozyme at two different ionic strengths (**Figure 5**).

HSA is the major protein present in human blood and will be one of the first components that interact with foreign

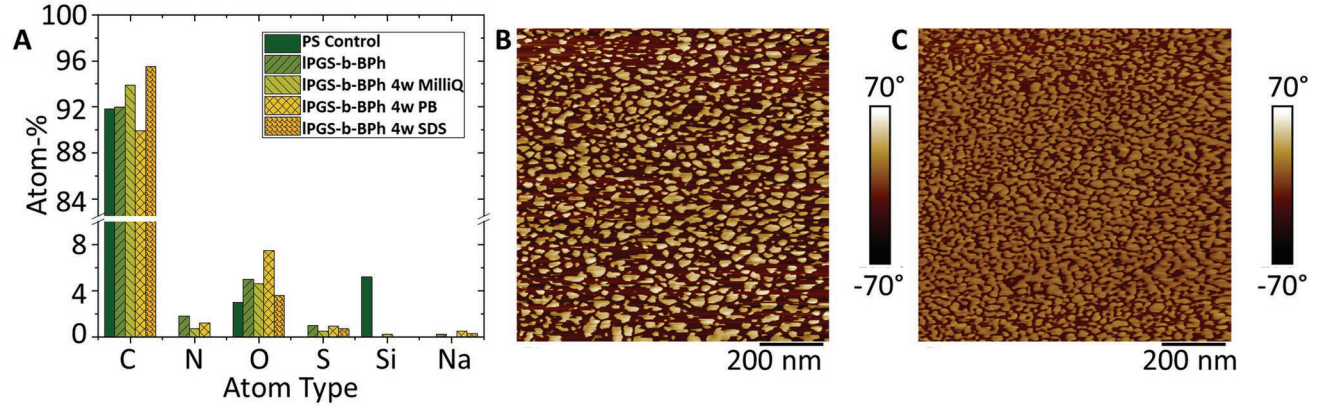

Figure 4. Stability experiments of lPGS-b-BPh coating on PS. A) XPS data of bare PS, untreated lPGS-b-BPh on PS, and coatings that have been incubated for 4 weeks either in MilliQ water, phosphate buffer (PB) with an ionic strength of 50×10^{-3} M, or 2% SDS solution. Nitrogen and sulfur content indicate the presence of lPGS-b-BPh on the surface. The polymer is still present after treatment with water or with PB. No nitrogen is detectable after SDS treatment, showing that the combination of high osmotic pressure and strong detergent remove the polyelectrolyte layer, likely together with the PS chains that are chemically linked to lPGS-b-BPh. B,C) Phase images of AFM measurements of surfaces treated with PB solution or MilliQ water. The treatment leads to a visible change in morphology of the coated surface, but not to a full removal of the polymer.

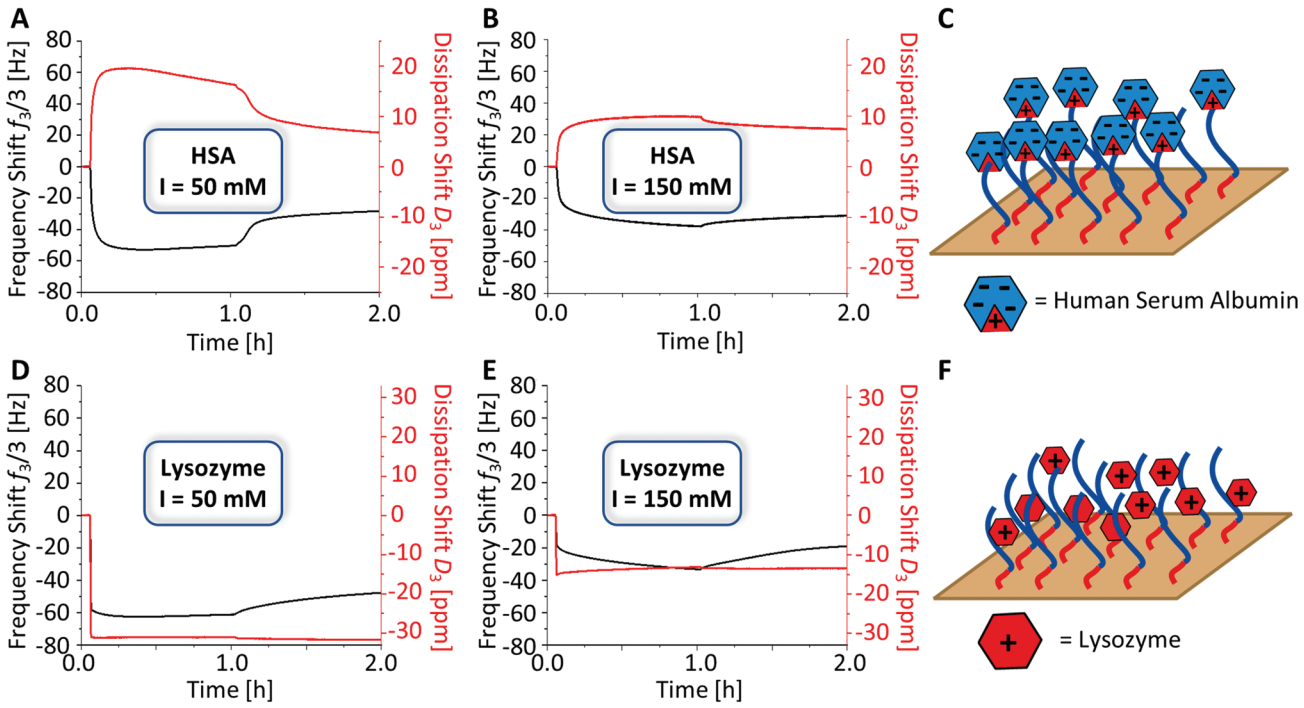

Figure 5. The binding of HSA and lysozyme to lPGS-b-BPh coated QCM-D chips. A,B) HSA binding at ionic strength of 50×10^{-3} and 150×10^{-3} M, respectively. The negative frequency shift and positive dissipation shift indicate that HSA binds primarily on top of the lPGS layer, adding a viscoelastic layer to the system (depicted schematically in C). D,E) Lysozyme binding at ionic strength of 50×10^{-3} and 150×10^{-3} M, respectively. In this case, frequency shift as well as dissipation shift are negative. The viscoelasticity of the system decreases while lysozyme adsorbs to the surface, indicating that the protein is penetrating the lPGS layer, thereby decreasing the flexibility of the polymer chains (depicted schematically in F).

surfaces. Although HSA is overall negatively charged, a significant amount of the protein is adsorbed to the surface (Figure 5A,B).[27,38] This counter-intuitive behavior can be explained by a positively charged patch on the protein surface, which is responsible for the binding.[39] The increase of dissipation in this case indicates that the protein binds on top of the polymer layer, adding to the overall thickness and viscoelasticity of surface-bound material (Figure 5C). Such behavior has been previously reported for a hPGS coated gold surface, and is also in excellent agreement to the results of Yigit et al. in a computer simulation study.[26,40] The applied ionic strengths had a minor effect on the rate of binding, and no effect on the overall amount of bound protein after buffer washing. This suggests that the binding on the surface of the polymer layer is independent of the conformational state of the lPGS chains.

We find that the coated surfaces bind roughly four times the mass of HSA as compared to a pure PS surface (Figure S3, Supporting Information). The comparison with the control measurement further confirms that the coated area of the surface is responsible for the protein binding, and HSA does not only bind to the PS surface in gaps between coated areas.

Lysozyme served as a model for a small, positively charged protein in this study.[41,42] The overall positive charge led to a strong binding to the negatively charged surface, as indicated by the drastic negative frequency shift (Figure 5D,E). In this case, the dissipation also exhibited a strong negative shift, which can be explained by proteins primarily penetrating the lPGS layer instead of binding on the surface (Figure 5F). The proteins inside the layer will likely be complexed by surrounding lPGS chains and thereby lead to a more collapsed, less viscoelastic state of the polymer layer. A similar behavior has been reported by Yang et al. for positively charged polyelectrolyte brushes and a negatively charged protein. In their study, bovine serum albumin (BSA) penetrated the polymer layer, yielding a negative frequency as well as negative dissipation shift in QCM-D experiments.[43] In the case of lysozyme on lPGS-b-BPh coated surfaces, the ionic strength had a significant impact. At an ionic strength of $I = 150 \times 10^{-3}$ M, less protein binds to the surface than at $I = 50 \times 10^{-3}$ M. This may be explained by the salted brush regime of the lPGS chains at higher ionic strength (see Figure 3) which diminishes the effect of counterion release.[27,42]

In summary, the QCM-experiments show that protein adsorption to the novel lPGS-b-BPh coated surface is in good agreement to expectations based on previous reports on comparable systems. Therefore, it may be a suitable surface coating to generate blood-compatible surfaces, which will be discussed in the following section.

2.6. Interaction of lPGS-b-BPh Coatings with Blood Serum

The complement system was chosen as a suitable target to test the effect of lPGS-b-BPh coated PS surfaces on blood serum.[44] It is an important part of the innate immune system and closely connected to inflammatory processes.[45] Polysulfates like heparin or dPGS reportedly reduce the complement activation.[44,46] Furthermore, the production as well as the activity

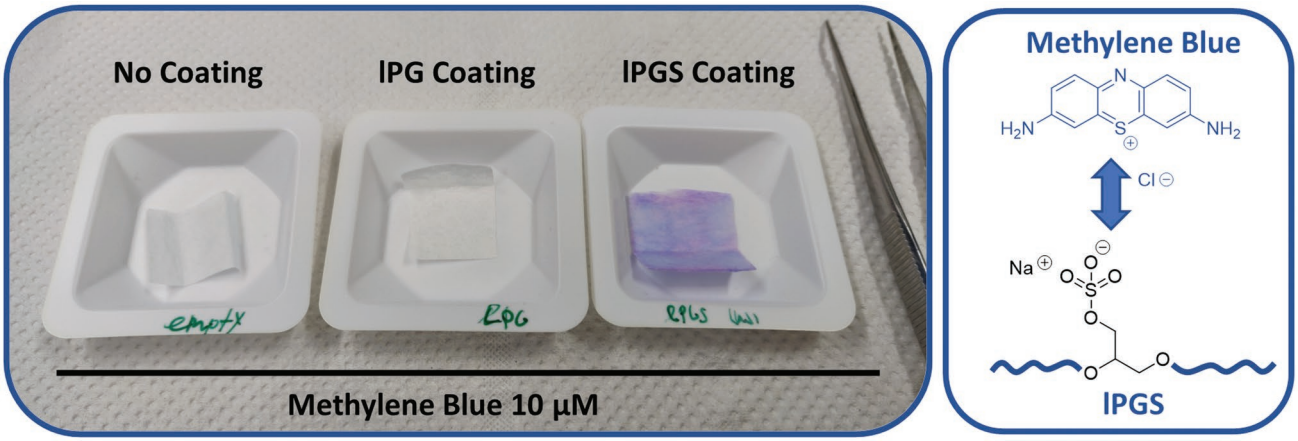

Figure 6. Polypropylene fleece incubated with the positively charged dye methylene blue. Fleece with no coating or with noncharged lPG-b-BPh coating do not bind the charged dye significantly. The lPGS-b-BPh coating results in a rapid uptake of the dye.

of the inflammation-mediating anaphylatoxins C3a and C5a are reduced when the complement system is inhibited by dPGS.[44] Hence, we tested if the complement activation of blood serum will be reduced after being in contact with lPGS-b-BPh coated surfaces.

Since we were restricted to the binding capacity of the given functionalized surfaces of 1 cm^2 per sample, several initial experiments of serum dilutions were performed to meet the effective range of detection (data not shown). Additionally, sufficient diluted serum volume was required to perform several replicate measurements.

Therefore, 150 µL of 10% serum was incubated with either an lPGS coated PS surface, or with a protein-repellent lPG coated PS surface as control.[33] After incubation, sera were collected. The residual activity of the mannose binding lectin (MBL) pathway of the complement system was determined by using a commercial enzyme-linked immunosorbent assay (ELISA) as described in the experimental section. As indicated by the manufacturer's instruction a further 10-fold dilution is required to meet the effective range. Untreated blood serum was used as control and normalized to 100% activity. Values of the surface incubated samples are given relative to the untreated control.

The lPG coated samples showed a residual activity of 92 ± 6%. This can be explained by the overall protein-repellent nature of the sample. In the case of lPGS, the complement activity was reduced to 78 ± 4%. Thus, electrostatic interactions obviously contribute to binding complement protein and lower the activity of the whole system. A comparable reduction of 22% complement activity of the Lectin pathway (MBL) was previously achieved with two soluble polysulfates, dendritic polyglycerolsulfate (dPGS) and linear heparin at an equal concentration of about 25×10^{-9} M (estimated from Silberreis et al., Figure 2).[44]

In this first experiment, it was demonstrated that lPG-b-BPh coated PS is a nearly bioinert surface and lPGS-b-BPh functionalization even bears the potential to reduce the complement activation. Further research is needed to substantiate this finding and evaluate the hemocompatibility in more detail, with respect to anti-inflammatory and anti-coagulation properties.

2.7. Applicability to a Different Polymer Material

The coating procedure for lPGS-b-BPh needs to be applicable to different polymer surfaces as well, considering the composition of many blood contacting medical devices. A common material is polypropylene. Therefore, we tested the coating procedure on a fleece material made of polypropylene. The success of the coating was demonstrated by applying a positively charged dye (methylene blue, MB) that will bind to the negatively charged sulfate groups on the polymer (**Figure 6**).

Fleece samples either without any coating, with a noncharged lPG-b-BPh coating, or with the lPGS-b-BPh coating, were immersed in an aqueous solution of MB (3 mL, $c = 10 \times 10^{-6}$ M). The samples were incubated for 24 h at room temperature and then washed thoroughly with water. Both control samples did not change color, while the lPGS coated fleece rapidly soaked up the dye from the solution.

This simple experiment demonstrates that the coating procedure can be applied to PP as well as PS. Based on this result, we expect that other common non-activated polymeric materials can be coated as well, giving rise to a broad applicability on medical devices.

3. Conclusion

In this study, we succeeded to develop a simple and robust method to prepare lPGS brush coatings on polystyrene. We synthesized an amphiphilic polyelectrolyte block copolymer consisting of lPGS and a benzophenone containing anchor block. We demonstrated that tuning the aggregation behavior with a chaotropic salt enabled the covalent attachment of the polymer on PS surfaces via UV crosslinking. The resulting layer exhibits an aggregate morphology on the coated surface and shows typical characteristics of a polyelectrolyte brush surface. The polymer chains stretch or collapse in response to different ionic strengths of the surrounding medium and are reasonably stable upon incubation with aqueous buffer solution over several weeks. Proteins will bind on or penetrate into the lPGS layer, depending on their surface charge. The comple-

ment activity of blood serum is reduced after in contact with the coated surface by 22%. Furthermore, we demonstrated that the coating procedure is not limited to PS but can perspectively be applied to a variety of non-activated polymer surfaces.

4. Experimental Section

Materials and Methods: All chemicals and solvents were obtained from commercial suppliers and used without further purification, unless stated otherwise. Air- and moisture-sensitive reactions were performed under argon atmosphere in flame-dried flasks. Light-sensitive reactions were performed either in brown-glass flasks or in flasks wrapped in aluminum foil. NMR data were recorded by the core facility BioSupraMol at Freie Universität Berlin on either a Bruker Avance III 700 MHz spectrometer (Bruker, MA, USA) or a JEOL ECA 600 MHz spectrometer (JEOL, Tokyo, Japan).

Synthesis of lPG-b-NH_2: The starting polymer lPG-b-NH_2 was synthesized as previously described.[33] In brief, a block copolymer of an acetal-protected glycidyl monomer (EEGE) and allyl glycidyl ether (AGE) was synthesized via ring-opening anionic polymerization. After acetal deprotection under acidic conditions, the allyl groups were coupled with cysteamine via thiol–ene reaction to yield the amine groups on the polymer.

Benzophenone Functionalization: The benzophenone functionalities were introduced by amide coupling of 4-benzoylbenzoic acid. lPG-b-NH_2 (250 mg, 0.25 mmol of NH_2 groups) was lyophilized from an aqueous stock solution and immediately dissolved in DMF (10 mL). Triethylamine (0.25 mL, 0.19 g, 1.5 mmol), NHS (45 mg, 0.38 mmol), EDCl (75 mg, 0.38 mmol), and 4-benzoylbenzoic acid (87 mg, 0.38 mmol) were added successively and the reaction mixture was stirred in the dark at room temperature for 18 h. Subsequently, the reaction mixture was diluted with 20 mL of methanol, and the product was purified by dialysis for 5 days (MeOH, RC dialysis tube, MWCO = 1 kDa). The content of benzophenone groups was determined by ^{1}H NMR spectroscopy.

^{1}H NMR (600 MHz, MeOD-d_4, δ): 8.03–7.53 (Ar—H, Benzophenone), 3.77–3.49 (CH_2—CH—CH_2, polymer backbone, O—CH_2—CH_2—CH_2—S), 2.85–2.30 (O—CH_2—CH_2—CH_2—S, S—CH_2—CH_2—N), 1.87 (O—CH_2—CH_2—CH_2—S) ppm.

Sulfation of lPG-b-BPh: The sulfation of lPG-b-BPh was carried out in a slightly modified version of a previously reported protocol.[22] lPG-b-BPh (250 mg, 3.4 mmol OH groups) was transferred from MeOH to DMF without drying it completely by repeatedly adding 10 mL DMF and evaporating most of the solvent. To the polymer solution, a solution of SO_3-pyridine complex (672 mg, 8.4 mmol) in 10 mL dry DMF was added dropwise over the course of 4 h at 60 °C under argon atmosphere. After complete addition of SO_3–pyridine, the reaction was stirred at 60 °C in the dark for 18 h. The mixture was cooled to room temperature, quenched by addition of 1 M NaOH, and the product was purified by dialysis for 7 d (brine → H_2O, RC dialysis tube, MWCO = 1 kDa). The polymer was characterized by NMR spectroscopy and GPC, and the success of the sulfation was determined by elemental analysis (degree of sulfation > 90%).

^{1}H NMR (700 MHz, D_2O, δ): 8.00–7.50 (Ar—H, Benzophenone), 4.33–3.98 (CH_2—CH—CH_2—OSO_3Na), 3.98–3.50 (CH_2—CH—CH_2, polymer backbone), 3.42–2.36 (O—CH_2—CH_2—CH_2—S, S—CH_2—CH_2—N), 2.02 (O—CH_2—CH_2—CH_2—S) ppm. Anal. calcd for lPGS-b-BPh: C 26.12, H 3.42, N 0.73, S 17.43; found: C 25.94, H 3.90, N 1.03, S 15.90. GPC: M_n = 47 kDa, M_w = 124 kDa, D = 2.60.

Quartz Crystal Microbalance with Dissipation: Quartz crystal microbalance measurements were performed using a QSense QCM-D system (Biolin Scientific, Gothenburg, Sweden). QCM sensors precoated with polystyrene were purchased from Biolin Scientific and cleaned according to the manufacturer's instructions prior to use. All measurements were performed at 20 °C and at a constant flow rate of 0.1 mL min^{-1}. During measurements, the base frequency was recorded as well as all odd-numbered overtones up to the 13th overtone. Due to their highest sensitivity, the 3rd up to 9th overtones were used for subsequent data analysis. Aqueous solutions used in QCM experiments were degassed by ultrasonication for 20 min. Protein solutions were prepared by dissolving the respective protein in a degassed aqueous buffer. For experiments that include UV irradiation, a window module supplied by Biolin Scientific was used, which is equipped with a sapphire window above the sensor surface.

Atomic Force Microscopy: Atomic force microscopy measurements were performed on a Multimode 8 atomic force microscope (Bruker, MA, USA) in tapping mode. The measurements were performed using PPP-NCLR cantilevers from Bruker with a force constant of 48 N m^{-1} and a resonance frequency of 190 kHz. Scan frequency and amplitude setpoint were adjusted to achieve a maximum resolution. Obtained images were analyzed using the software NanoScope Analysis from Bruker (version 1.5) and processed using 1st order flattening and plane fit. Analysis of the size and thickness of coated areas was performed using the particle analysis function within the software.

Dynamic Light Scattering: Dynamic light scattering experiments were performed using a Zetasizer Ultra (Malvern Panalytical Ltd., Malvern, United Kingdom) in backscattering mode (detection angle = 173°) at a constant temperature of T = 20 °C. For DLS measurements, disposable plastic cuvettes with a volume of 70 µL were used, and all solutions were filtered through a 0.2 µm syringe filter directly before the measurement to remove any dust particles from the solutions. Each measurement was continued until at least 20 single measurement runs of adequate quality were recorded. Data evaluation was performed using the software ZS Xplorer (Malvern Panalytical Ltd., Malvern, United Kingdom).

General Procedure of Offline Coatings: The coating with lPGS-b-BPh was performed on silicon wafers (1 × 1 cm^2) that had been spin-coated with a layer of approximately 100 nm polystyrene. The wafers were immersed in 1.9 mL solution of guanidine hydrochloride (1 M) for 20 min. By adding 0.1 mL stock solution of lPGS-b-BPh (2 mg mL^{-1}), the coating solution was prepared with a final concentration of 0.1 mg mL^{-1} for lPGS-b-BPh and 0.95 M guanidine hydrochloride. After 20 min incubation, the solution was removed, the wafers were washed with 1 M guanidine hydrochloride, and then irradiated with UV light (366 nm, UV lamp from Camag, Germany) for 10 min. The wafers were again washed with 1 M guanidine hydrochloride solution, then with buffered salt solution (5×10^{-3} M phosphate buffer with added NaCl to achieve an overall ionic strength of 50×10^{-3} M), then with MilliQ water and were blow dried in a stream of dry nitrogen.

Preparation of Polystyrene Coated Silicon Wafers: Silicon wafers of 1 × 1 cm^2 were coated with a homogeneous layer of polystyrene via spin coating. Initially, all wafers were cleaned in toluene ultrasonically for at least 10 min. After rinsing with plenty ethanol and water, they were blow dried in a stream of dry nitrogen gas. The wafers were placed in a spin coater of Laurell Technologies Corp. (Pennsylvania, USA, model WS-650MZ-23NPPB) immediately, and coated with a solution of polystyrene in toluene (2 wt%, 50 µL) at a rotation speed of 3000 rpm for 60 s. After drying the wafers thoroughly in a drying oven at 60 °C, the polystyrene layer thickness on each wafer was measured individually using ellipsometry.

Ellipsometry: Ellipsometric dry thickness was determined using a SENpro spectroscopic ellipsometer from SENTECH Instruments GmbH (Berlin, Germany) at an incident angle of 70° and a wavelength spectrum from 400 to 800 nm. For each coating experiment, at least three independent surfaces were used, and on each surface, at least three different spots were measured.

Contact Angle: Contact angle measurements were performed on the contact angle goniometer OCA20 (Dataphysics Instruments, Filderstadt, Germany) by gently placing a droplet of 2 µL MilliQ grade water on top of the surface and recording the droplet shape with a camera. After equilibration for 10 s, the contact angle was determined via the software SCA20 (Dataphysics Instruments, Filderstadt, Germany). Captive bubble contact angles were measured in MilliQ water with a 10 µL air bubble.

X-Ray Photoelectron Spectroscopy: X-ray photoelectron spectroscopy (XPS) spectra were recorded on a Kratos (Manchester, UK) Axis Ultra DLD spectrometer, equipped with a monochromatic Al Kα X-ray source.

The spectra were measured in normal emission, and a source-to-sample angle of 60° was used. All spectra were recorded utilizing the fixed analyzer transmission (FAT) mode. The binding energy scale of the instrument was calibrated, following a technical procedure provided by Kratos Analytical Ltd (calibration was performed according to ISO 15472). The spectra were recorded utilizing the instrument's slot and hybrid lens modes. An analysis area of approximately 300 µm × 700 µm was investigated; charge neutralization was applied. For quantification, the survey spectra were measured with a pass energy of 80 eV, and the spectra were quantified utilizing the empirical sensitivity factors that were provided by KRATOS (the sensitivity factors were corrected with the transmission function of the spectrometer).

Cryo-TEM Measurements: A solution of lPGS-b-BPh with Cs^+ ions was prepared by dialysis (MWCO 100–500 Da, CE tubing) in an aqueous solution of CsCl (0.5 M) for 24 h. Excess salt was removed by dialyzing in pure water for 24 h. The sample was freeze-dried and dissolved in pure water to a final polymer concentration of 1 mg mL^{-1}. Droplets (4 µL) of the sample solution were placed on hydrophilized holey carbon filmed grids (Quantifoil R1/2) at room temperature. The excess fluid was blotted off using filter paper to generate an ultrathin layer of the solution (typical thickness around 100 nm) spanning the holes in the carbon film. The grids were vitrified in liquid ethane using an automated vitrification robot (FEI Vitrobot Mark III) and stored in liquid nitrogen prior to the measurement.

The vitrified grids were stabilized by a copper autogrid and fixed with a spring clamp under liquid nitrogen. These autogrids were transferred under liquid nitrogen into a Talos Arctica transmission electron microscope (ThermoFisher Scientific Inc., Waltham, MA, USA) using the microscope's autoloader transfer routine.

Micrographs were recorded using the microscopes low-dose protocol at a primary magnification of 28000× and an acceleration voltage of 200 kV. Images were recorded by a Falcon 3CE direct electron detector (48 aligned frames) at full size (4k). The defocus was chosen to be 5 µm in all cases to create sufficient phase contrast.

Complement Activation Assay: To analyze complement activity the Wieslab Complement MBL Pathway ELISA (Svar Life Science, Malmö, Sweden) was applied following the given instructions for use. The assay is normally applied to detect immuno-compromised patients with a reduced MBL pathway activity. Here one adapted the assay with slight modifications in the preanalytical phase to demonstrate, if the surface modification reduces the fully activated state of the cascade, which would be beneficial in an application like coating of medical devices. In detail, the provided positive control human serum was prediluted in phosphate buffered saline (PBS) to 10%. Surfaces of 1 cm^2 were put in a 24 well plate (Corning Life Sciences, Schiphol, The Netherlands), initially washed with 500 µL PBS and covered with 150 µL diluted serum for 5 min at room temperature and constant slow shaking. Harvested serum was then further diluted 10-fold with the provided dilution buffer. The ELISA protocol in brief: 100 µL of the diluted serum (now 1%) was finally transferred to each well to initiate the complement cascade reactions. Terminal complex (pore) formation was quantified via an antibody enzyme-conjugate that converts a colorless substrate into a stable dye. Absorption was read in an Infinite 200 PRO microplate reader (Tecan, Männedorf, Switzerland) at 405 nm. Measurements were performed in triplicate and repeated two times.

Coating on Polypropylene and Detection with Methylene Blue: Polypropylene fleece samples (≈1.5 × 1.5 cm^2) were obtained from the inner melt-blown layer of commercial medical face masks. The lPGS-b-BPh coating was performed analogous to the standard procedure on PS. The fleece samples were initially immersed in aqueous GHCl solution and ultrasonicated for 5–10 s to ensure complete soaking of the fleece. After polymer incubation and washing, both sides of the fleece were each irradiated with UV light for 5 min. Fleece samples either without coating, with lPG coating, or with lPGS coating were immersed in a solution of methylene blue (3 mL each, $c = 10 \times 10^{-6}$ M) and incubated for 24 h at room temperature. The uncoated and lPGS coated samples were ultrasonicated for a few seconds in the beginning to ensure complete soaking of the fleece. After incubation, the samples were washed with water thoroughly and dried at 60 °C.

Supporting Information

Supporting Information is available from the Wiley Online Library or from the author.

Acknowledgements

The authors thank D. Kutifa (Freie Universität Berlin) for synthesizing the starting polymer lPG-b-NH_2. J. Walkowiak (Aachen-Maastricht Institute for Biobased Materials, Maastricht University) is gratefully thanked for extensive discussions on the evaluation of QCM-D data. The assistance of the BioSupraMol core facility (located at the Freie Universität Berlin and supported by the Deutsche Forschungsgemeinschaft) is acknowledged for the characterization of the used polymeric materials. The authors gratefully thank the BMBF for financial support in the project PathoClear.

Open access funding enabled and organized by Projekt DEAL.

Conflict of Interest

The authors declare no conflict of interest.

Data Availability Statement

The data that support the findings of this study are available in the supplementary material of this article.

Keywords

blood compatibility, Hofmeister series, linear polyglycerol sulfate, polyelectrolyte brushes, quartz crystal microbalance, surface coatings

Received: October 14, 2021
Revised: November 24, 2021
Published online: January 17, 2022

[1] I. H. Jaffer, J. I. Weitz, *Acta Biomater.* **2019**, *94*, 2.
[2] J. L. Brash, T. A. Horbett, R. A. Latour, P. Tengvall, *Acta Biomater.* **2019**, *94*, 11.
[3] Q. Wei, T. Becherer, S. Angioletti-Uberti, J. Dzubiella, C. Wischke, A. T. Neffe, A. Lendlein, M. Ballauff, R. Haag, *Angew. Chem., Int. Ed.* **2014**, *53*, 8004.
[4] B. K. D. Ngo, M. A. Grunlan, *ACS Macro Lett.* **2017**, *6*, 992.
[5] L. Yuan, Q. Yu, D. Li, H. Chen, *Macromol. Biosci.* **2011**, *11*, 1031.
[6] R. Gbyli, A. Mercaldi, H. Sundaram, K. A. Amoako, *Adv. Mater. Interfaces* **2018**, *5*, 1700954.
[7] M. Hedayati, M. J. Neufeld, M. M. Reynolds, M. J. Kipper, *Mater. Sci. Eng., R* **2019**, *138*, 118.
[8] M. F. Maitz, M. C. L. Martins, N. Grabow, C. Matschegewski, N. Huang, E. L. Chaikof, M. A. Barbosa, C. Werner, C. Sperling, *Acta Biomater.* **2019**, *94*, 33.
[9] M. Amiji, K. Park, *J. Biomater. Sci., Polym. Ed.* **1993**, *4*, 217.
[10] I. Banerjee, R. C. Pangule, R. S. Kane, *Adv. Mater.* **2011**, *23*, 690.
[11] L. Hong, Z. Wang, X. Wei, J. Shi, C. Li, *J. Pharmacol. Toxicol. Methods* **2020**, *102*, 106678.
[12] H. F. Haddad, J. A. Burke, E. A. Scott, G. A. Ameer, *Regener. Eng. Transl. Med.* **2021**, https://doi.org/10.1007/s40883-021-00198-y.
[13] G. T. Kozma, T. Shimizu, T. Ishida, J. Szebeni, *Adv. Drug Delivery Rev.* **2020**, *154-155*, 163.
[14] P. Sellaturay, S. Nasser, P. Ewan, *J. Allergy Clin. Immunol. Pract.* **2021**, *9*, 670.

[15] R. Biran, D. Pond, *Adv. Drug Delivery Rev.* **2017**, *112*, 12.
[16] L. E. Collins, L. Troeberg, *J. Leukocyte Biol.* **2019**, *105*, 81.
[17] S. N. Baytas, R. J. Linhardt, *Drug Discovery Today* **2020**, *25*, 2095.
[18] E. Vilanova, A. M. F. Tovar, P. A. S. Mourão, *J. Thromb. Haemostasis* **2019**, *17*, 254.
[19] J. Y. Van Der Meer, E. Kellenbach, L. J. van den, *Bos, Molecules* **2017**, *22*, 1025.
[20] A. Al Nahain, V. Ignjatovic, P. Monagle, J. Tsanaktsidis, V. Ferro, *Med. Res. Rev.* **2018**, *38*, 1582.
[21] C. Cheng, S. Sun, C. Zhao, *J. Mater. Chem. B* **2014**, *2*, 7649.
[22] H. Türk, R. Haag, S. Alban, *Bioconjugate Chem.* **2004**, *15*, 162.
[23] N. Rades, K. Licha, R. Haag, *Polymers* **2018**, *10*, 595.
[24] J. Dernedde, A. Rausch, M. Weinhart, S. Enders, R. Tauber, K. Licha, M. Schirner, U. Zugel, A. von Bonin, R. Haag, *Proc. Natl. Acad. Sci. USA* **2010**, *107*, 19679.
[25] S. Reimann, D. Gröger, C. Kühne, S. B. Riese, J. Dernedde, R. Haag, *Adv. Healthcare Mater.* **2015**, *4*, 2154.
[26] D. D. Stöbener, F. Paulus, A. Welle, C. Wöll, R. Haag, *Langmuir* **2018**, *34*, 10302.
[27] J. Walkowiak, M. Gradzielski, S. Zauscher, M. Ballauff, *Polymers* **2020**, *13*, 122.
[28] M. Biesalski, D. Johannsmann, J. Rühe, *J. Chem. Phys.* **2002**, *117*, 4988.
[29] T. Ameringer, F. Ercole, K. M. Tsang, B. R. Coad, X. Hou, A. Rodda, D. R. Nisbet, H. Thissen, R. A. Evans, L. Meagher, J. S. Forsythe, *Biointerphases* **2013**, *8*, 16.
[30] J. O. Zoppe, N. C. Ataman, P. Mocny, J. Wang, J. Moraes, H. A. Klok, *Chem. Rev.* **2017**, *117*, 1105.
[31] M. Fromel, D. M. Sweeder, S. Jang, T. A. Williams, S. H. Kim, C. W. Pester, *ACS Appl. Polym. Mater.* **2021**, 3, 5291.
[32] S. Das, M. Banik, G. Chen, S. Sinha, R. Mukherjee, *Soft Matter* **2015**, *11*, 8550.
[33] L. Yu, Y. Hou, C. Cheng, C. Schlaich, P.-L. M. Noeske, Q. Wei, R. Haag, *ACS Appl. Mater. Interfaces* **2017**, *9*, 44281.
[34] L. Yu, C. Cheng, Q. Ran, C. Schlaich, P. L. M. Noeske, W. Li, Q. Wei, R. Haag, *ACS Appl. Mater. Interfaces* **2017**, *9*, 6624.
[35] M. Ballauff, O. Borisov, *Curr. Opin. Colloid Interface Sci.* **2006**, *11*, 316.
[36] B. Kang, H. Tang, Z. Zhao, S. Song, *ACS Omega* **2020**, *5*, 6229.
[37] F. Hofmeister, *Arch. Exp. Pathol. Pharmakol.* **1888**, *25*, 1.
[38] Q. Ran, X. Xu, P. Dey, S. Yu, Y. Lu, J. Dzubiella, R. Haag, M. Ballauff, *J. Chem. Phys.* **2018**, *149*, 163324.
[39] K. Achazi, R. Haag, M. Ballauff, J. Dernedde, J. N. Kizhakkedathu, D. Maysinger, G. Multhaup, *Angew. Chem., Int. Ed.* **2021**, *60*, 3882.
[40] C. Yigit, M. Kanduč, M. Ballauff, J. Dzubiella, *Langmuir* **2017**, *33*, 417.
[41] Q. Ran, X. Xu, J. Dzubiella, R. Haag, M. Ballauff, *ACS Omega* **2018**, *3*, 9086.
[42] J. J. Walkowiak, M. Ballauff, R. Zimmermann, U. Freudenberg, C. Werner, *Biomacromolecules* **2020**, *21*, 4615.
[43] J. Yang, Z. Hua, T. Wang, B. Wu, G. Liu, G. Zhang, *Langmuir* **2015**, *31*, 6078.
[44] K. Silberreis, N. Niesler, N. Rades, R. Haag, J. Dernedde, *Biomacromolecules* **2019**, *20*, 3809.
[45] M. Noris, G. Remuzzi, *Semin. Nephrol.* **2013**, *33*, 479.
[46] R. J. Linhardt, T. Toida, *Acc. Chem. Res.* **2004**, *37*, 431.